

---

---

# Relationship Between $^{18}\text{F}$ -FDG Accumulation and Lactate Dehydrogenase A Expression in Lung Adenocarcinomas

Xiang Zhou\*<sup>1</sup>, Ruohua Chen\*<sup>1</sup>, Wenhui Xie<sup>2</sup>, Yicheng Ni<sup>3</sup>, Jianjun Liu<sup>1</sup>, and Gang Huang<sup>1,4</sup>

<sup>1</sup>Department of Nuclear Medicine, Ren ji Hospital, School of Medicine, Shanghai Jiao Tong University, Shanghai, China;

<sup>2</sup>Department of Nuclear Medicine, Shanghai Chest Hospital, School of Medicine, Shanghai Jiao Tong University, Shanghai, China;

<sup>3</sup>Theragnostic Laboratory, Department of Imaging and Pathology, Faculty of Medicine, KU Leuven, Belgium; and <sup>4</sup>Department of Cancer Metabolism, Institute of Health Sciences, Chinese Academy of Sciences and Shanghai Jiao Tong University School of Medicine, Shanghai, China

---

$^{18}\text{F}$ -FDG PET has been widely used in the management of malignant tumors. Lactate dehydrogenase A (LDHA) plays an important role in the development, invasion, and metastasis of malignancies. However, the relationship between  $^{18}\text{F}$ -FDG accumulation and LDHA expression has not been investigated. **Methods:** Retrospective analysis was conducted for 51 patients with lung adenocarcinomas who underwent  $^{18}\text{F}$ -FDG PET. The relationship between maximum standardized uptake value and the expression of LDHA, glucose transporter 1 (GLUT1), and hexokinase 2 (HK2) were examined. RNA interference was used to analyze the role of LDHA in tumor metabolism and growth in A549 cells. The AKT, also known as protein kinase B, pathway was also investigated to evaluate the molecular mechanisms of the relationship between LDHA expression and  $^{18}\text{F}$ -FDG uptake. **Results:** Maximum standardized uptake value was significantly higher in the LDHA high-expression group than the LDHA low-expression group ( $P = 0.018$ ). GLUT1 expression in lung adenocarcinomas was positively correlated with  $^{18}\text{F}$ -FDG accumulation and LDHA expression whereas HK2 expression was not. Knockdown of LDHA led to a significant decrease in GLUT1 expression,  $^{18}\text{F}$ -FDG uptake, and cell proliferation. The activated form of AKT was also decreased after LDHA knockdown. **Conclusion:** LDHA increases  $^{18}\text{F}$ -FDG accumulation into non-small cell lung cancer, possibly by upregulation of GLUT1 expression but not HK2 expression. LDHA may modulate  $^{18}\text{F}$ -FDG uptake in lung adenocarcinomas via the AKT-GLUT1 pathway. These results indicate that  $^{18}\text{F}$ -FDG PET/CT may predict LDHA expression levels and response to anti-LDHA therapy in lung adenocarcinomas.

**Key Words:** lung adenocarcinomas; LDHA; GLUT1; glycolysis;  $^{18}\text{F}$ -FDG uptake

**J Nucl Med 2014; 55:1766–1771**

DOI: 10.2967/jnumed.114.145490

Lung cancer is the most prevalent and lethal malignant tumor in the world (1,2), among which adenocarcinoma is the most common histologic type and could account for the increasing incidence of lung cancer to a large extent (3). Surgery and chemotherapy are 2 common strategies for its treatment (4,5). However, its rapid progression, high metastasis rate, and profound chemoresistance make this fatal disease difficult to treat (6). The TNM classification has been widely used in the clinical setting to estimate prognosis and for decision-making regarding treatment (7). However, this well-known classification could not provide information about biologic behavior of tumors and predict the prognosis of patients with lung cancer accurately (8,9). Therefore, interest in identifying and validating new molecular markers to better provide biologic profiles of non-small cell lung cancer and to identify patients at risk for poor prognosis is growing.

$^{18}\text{F}$ -FDG PET/CT is a less invasive diagnostic tool widely used in the diagnosis and staging of malignant tumors (10–12), especially lung cancer (13,14). Because tumor cells depend on glucose metabolism as a major energy substrate, increased  $^{18}\text{F}$ -FDG uptake on PET scans is known to be an indicator of the poor prognosis and aggressiveness of various tumors (15). The main mechanisms of  $^{18}\text{F}$ -FDG uptake in tumor cells are increased expression of the facilitated glucose transporters including type 1 (GLUT1) on the cell membrane and rate-limiting glycolytic enzymes, such as hexokinase 2 (HK2) (15,16).

The preference of cancer cells to produce energy by a high rate of glycolysis followed by lactic acid fermentation, even under adequate oxygen, has been called the Warburg effect (17,18). Compared with normal cells, tumor cells use more glucose through insufficient energy metabolism with production of lactate instead of using oxidative phosphorylation. Lactate dehydrogenase A (LDHA), which converts pyruvate to lactate, is overexpressed in many human cancers, compared with normal tissues (19). Upregulation of LDHA ensures efficient glycolytic metabolism for tumor cells and reduces oxygen dependency (20). We and others have demonstrated that LDHA plays an important role in the development, invasion, and metastasis of malignant tumors (21,22). However, the relationship between  $^{18}\text{F}$ -FDG accumulation and LDHA expression, and its possible mechanism, is not clear.

The current study aimed to investigate whether the protein expressions of LDHA, GLUT1, and HK2 are correlated with the  $^{18}\text{F}$ -FDG accumulation on PET images in lung adenocarcinomas using immunohistochemical analysis. In addition, we examined whether LDHA expression correlates with GLUT1 or HK2 and

---

Received Jul. 11, 2014; revision accepted Sep. 5, 2014.

For correspondence or reprints contact either of the following:  
Gang Huang, Department of Nuclear Medicine, Ren ji Hospital, School of Medicine, Shanghai Jiao Tong University, 1630 Dongfang Rd., Shanghai 200127, China.

E-mail: huang2802@163.com

Jianjun Liu, Department of Nuclear Medicine, Ren ji Hospital, School of Medicine, Shanghai Jiao Tong University, 1630 Dongfang Rd., Shanghai 200127, China.

E-mail: ljsh@133sh.com

\*Contributed equally to this work.

Published online Oct. 23, 2014.

COPYRIGHT © 2014 by the Society of Nuclear Medicine and Molecular Imaging, Inc.

**TABLE 1**  
Relationship Between LDHA Expression and Tumor Characteristics, Based on Immunohistochemical Score

Characteristic	No. of patients ( <i>n</i> = 51)		<i>P</i>
	Low ( <i>n</i> = 25)	High ( <i>n</i> = 26)	
Mean age ± SD (y)	68.2 ± 9.2	66.3 ± 9.1	0.231
Sex			0.691
Male	15	17	
Female	10	9	
Histologic type			0.029
Well/moderate	19	12	
Poor	6	14	
T category			0.002
Tis, T1, T2	21	11	
T3, T4	4	15	
N category			0.428
Negative	18	16	
Positive	7	10	
M category			0.952
Negative	21	22	
Positive	4	4	
Tumor size (cm)			0.048
≤3	20	14	
>3	5	12	
SUV <sub>max</sub>			0.018
Mean ± SD	7.048 ± 4.4773	10.062 ± 4.3191	

molecular mechanisms of knockdown of LDHA related to cellular inhibition and reduced <sup>18</sup>F-FDG uptake. In this study, we elucidated the relationship between LDHA expression and <sup>18</sup>F-FDG uptake and possible mechanisms of knockdown of LDHA related to cellular inhibition and decreased <sup>18</sup>F-FDG uptake.

## MATERIALS AND METHODS

### Study Population

Fifty-one patients (32 men and 19 women; age range, 43–86 y; mean age, 67 y) with lung adenocarcinomas were included in this study. They all underwent <sup>18</sup>F-FDG PET/CT scans before tumor resection at Shanghai Jiaotong University–affiliated Ren ji Hospital between December 2006 and December 2009. The following were eligibility criteria: the diagnosis of lung adenocarcinomas was confirmed by pathologic examination of surgical specimens; patients did not receive chemotherapy/radiotherapy before PET/CT scanning; complete case records including age, sex, tumor stage, and histologic differentiation were available; tissue specimens for immunohistochemical staining were available. Finally, 51 patients were evaluated in this study. The institutional review board of Shanghai Jiao Tong University–affiliated Ren ji Hospital approved this study, and all subjects signed a written informed consent form.

### PET/CT Imaging

Images were acquired with an integrated PET/CT device (Biograph HD 64; Siemens). PET was performed to cover the identical axial field of view after CT scanning. PET image datasets were reconstructed iteratively with CT data for attenuation correction. For quantitative analysis, irregular regions of interest were placed over the most intense area of <sup>18</sup>F-FDG accumulation. The maximum standardized

uptake value (SUV<sub>max</sub>) was calculated using the following formula: maximum pixel value with the decay-corrected region-of-interest activity (MBq/kg)/(injected dose [MBq]/body weight [kg]). The PET images were evaluated by 2 experienced nuclear medicine physicians.

### Immunohistochemistry

Biopsies taken from tumor resections were frozen in liquid nitrogen and stored at –80°C. Five-micrometer formalin-fixed paraffin sections were used for immunohistochemical staining with anti-GLUT1, anti-HK2, and anti-LDHA antibodies. All primary antibodies were purchased from Abcam. Immunohistochemical analyses were conducted by 2 board-certified pathologists. The slides were scored for intensity of staining (0–3).

### Cell Culture and Viability Assay

A549 cells (human lung adenocarcinoma cell line) were obtained from the Chinese Academy of Sciences and grown in Dulbecco modified Eagle medium (DMEM) (GIBCO) supplemented with 10% fetal bovine serum (GIBCO), penicillin (100 mg/mL), and streptomycin sulfate (100 mg/mL) (GIBCO) at 37°C and 5% CO<sub>2</sub>. The hypoxic conditions (1% O<sub>2</sub>) were maintained in a controlled-atmosphere chamber (Thermo Electron) at 37°C in certified 5% CO<sub>2</sub>/94% nitrogen. Lipofectamine 2000 (Invitrogen) was used in transient transfection according to the manufacturer's protocol. The LDHA–small-interference RNA (siRNA) and control were purchased from Pharma China. The following are the 2 targeting sequences for LDHA: LDHA-si1 sequence, GGCAAA-GACUAUAAUGUAA; LDHA-si2 sequence, AAAGUCUUCUGAUGUCAUA. In this study, the term LDHA-si1 is used to mean only 1 LDHA-si.

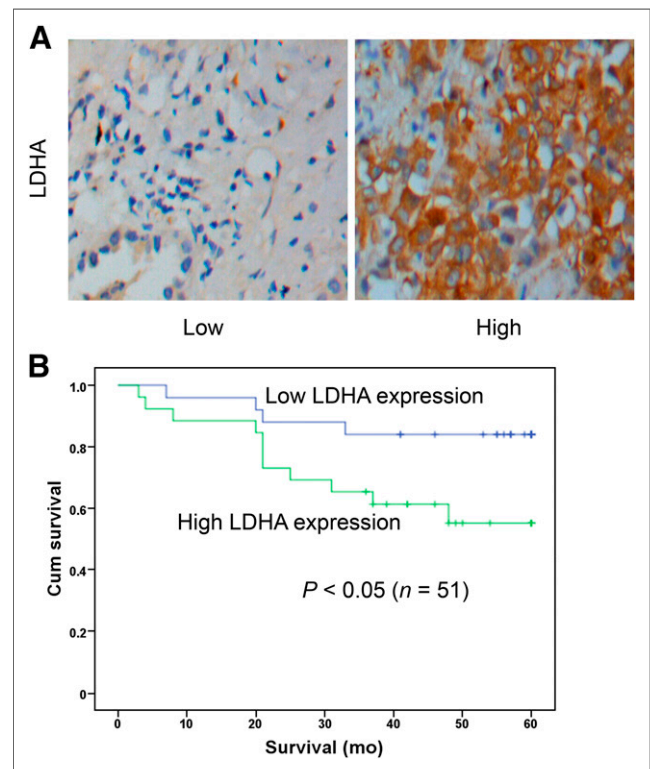


**FIGURE 1.** LDHA expression in lung adenocarcinomas is associated with poor prognosis. Fifty-one clinical human lung adenocarcinomas cases were subjected to immunohistochemical analyses with anti-LDHA antibody. Representative images from tissues with different LDHA scores are shown. (A) LDHA expression in representative tumor tissues ( $\times 400$ ). (B) Kaplan–Meier analysis of survival in 51 patients with lung adenocarcinomas stratified by LDHA expression level. Log-rank test showed significant differences between groups ( $P < 0.05$ ). Cum = cumulative.

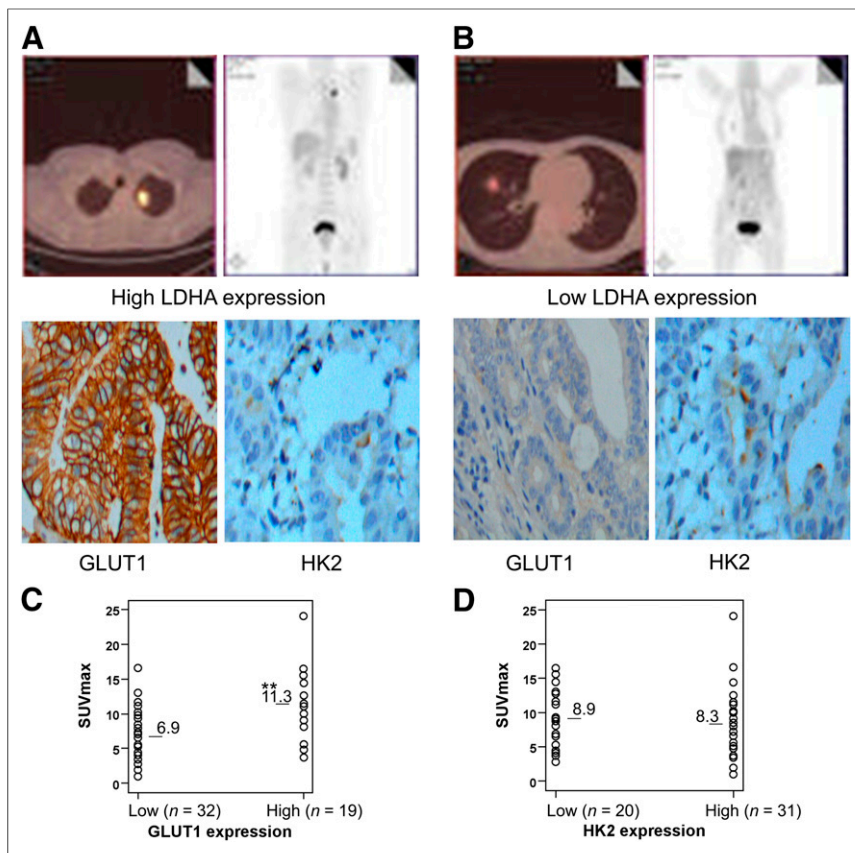


**FIGURE 2.** Correlation between  $^{18}\text{F}$ -FDG accumulation and expression of GLUT1 and HK2. (A) A 66-y-old man had left lung adenocarcinoma with high LDHA expression.  $^{18}\text{F}$ -FDG PET/CT scans showed intense accumulation of  $^{18}\text{F}$ -FDG in tumor ( $\text{SUV}_{\text{max}}$ , 16.5; TNM stage, T3N0M1). Immunohistochemical analysis revealed high GLUT1 expression and high HK2 expression in tumors. (B) A 54-y-old man had right lung adenocarcinoma with low LDHA expression.  $^{18}\text{F}$ -FDG PET/CT scans showed modest accumulation of  $^{18}\text{F}$ -FDG in tumor ( $\text{SUV}_{\text{max}}$ , 4.8; TNM stage, T2N0M0). Immunohistochemical analysis revealed low GLUT1 expression and high HK2 expression in tumors. (C) Correlation between  $^{18}\text{F}$ -FDG accumulation and GLUT1 expression.  $\text{SUV}_{\text{max}}$  was significantly higher in tumors with high GLUT1 expression than in those with moderate and low GLUT1 expression (\*\* $P < 0.01$ ). (D) Correlation between  $^{18}\text{F}$ -FDG accumulation and HK2 expression. HK2 expression in tumors was not correlated with  $\text{SUV}_{\text{max}}$  ( $P > 0.05$ ).

The cell survival rate was examined using a Cell Counting Kit-8 (Dojindo Molecular Technologies) (23). Cells were plated in 96-well plates at 6,000 cells/well. After 24 h of culture, transfection was performed using siRNA according to the manufacturer's protocol. For drug treatment, the medium was replaced with DMEM containing 0 or 10 mM oxamate. After incubation for 24–48 h, 10  $\mu\text{L}$  of CCK-8 was added to each well, and cells were further incubated for 2 h. Absorbance was read at 450 nm using an enzyme microplate reader. The half-maximal inhibitory concentration (IC50) value was calculated using GraphPad Prism (version 5.0; GraphPad Software). All experiments were performed in independent triplicate experiments.

#### Cell Metabolism Assay

To study the change of cell metabolism, we measured cellular adenosine triphosphate (ATP) level, cellular uptake of glucose, and lactate production.

Relative cellular ATP content was measured using the ATP bioluminescent somatic cell assay kit (Sigma) according to the manufacturer's instructions. Briefly,  $2 \times 10^5$  cells were seeded in a 24-well plate. After 24 h, cells were washed, centrifuged, and lysed. Lysates were collected, and luminescence was measured using a luminescence reader and

normalized to the protein concentration. Measurements were performed in triplicate.

$^{18}\text{F}$ -FDG cellular uptake can evaluate glucose uptake capacity of tumor cells. Cells were cultured in 12-well cell culture plates and then detached, washed twice, and subsequently incubated in 500  $\mu\text{L}$  of DMEM containing  $^{18}\text{F}$ -FDG (148 kBq [4  $\mu\text{Ci}/\text{mL}$ ]) for 1 h at 37°C. Pellets were then washed twice with ice-cold phosphate-buffered saline (PBS). Lysates were produced using 500  $\mu\text{L}$  of 0.1 M NaOH, and then the radioactivity of the whole-cell lysates was assayed using a well  $\gamma$  counter. These readouts were normalized to corresponding protein amounts (Beyotime). All experiments were performed in independent triplicate experiments.

Lactate levels in medium were measured using a lactate assay kit (CMA; Microdialysis). Cells were seeded onto 6-well plates and transfected with LDHA siRNA or oxamate. Approximately 48 h after transfection, cells were washed and cultured in serum-free DMEM for approximately 16 h (24). Lactate production was evaluated by assessing the lactate content in the culture medium by incubation in the presence of LDH and  $\text{NAD}^+$  and measuring nicotinamide adenine dinucleotide hydrogen formation at 340 nm. These readouts were normalized to corresponding protein amounts (Beyotime). Measurements were performed in triplicate.

#### Western Blot Analysis

Cells were harvested and lysed in a buffer containing 50 mM Tris-HCl, 150 mM NaCl, 2 mM ethylenediaminetetraacetic acid, 1% Triton, and 1 mM phenylmethanesulfonyl fluoride (Sigma) for 10 min on ice. Total proteins were extracted from the lysate, and protein concentrations were determined by the bicinchoninic acid protein assay. The proteins were fractionated using sodium dodecylsulfate polyacrylamide gel electrophoresis. Then proteins were transferred onto nitrocellulose membrane for Western blot as described earlier. The membranes were incubated about 3 h at 37°C with the primary antibodies in PBS with 5% nonfat milk. The following primary antibodies were used: anti-LDHA rabbit antibody (1:1,000; Abcam), anti-GLUT1 rabbit antibody (1:1,000; Abcam), anti-TIGAR rabbit antibody (1:500; Abcam), anti-TIGAR rabbit antibody (1:500; Abcam), anti-HK2 rabbit antibody (1:1,000; Abcam), anti-PKM2 rabbit antibody (1:1,000; Abcam), anti-AKT (AKT is also known as protein kinase B) rabbit antibody (1:2,000; Cell Signaling), anti-pAKT rabbit antibody (1:2,000; Cell Signaling), and anti- $\beta$ -actin antibody (1:2,000; Sigma). Membranes were extensively washed with PBS and incubated with secondary antirabbit antibody (1:10,000; LI-COR Biosciences). After washes with PBS, protein bands were scanned and analyzed using a Gel Doc XR system (Bio-Rad) and analyzed using IMAGE LABTM software (version 2.0; Bio-Rad).

#### Statistical Analysis

The data were shown as mean  $\pm$  SD. Statistical differences between the groups were compared using 1-way ANOVA and *t* tests. A *P* value of less than 0.05 was considered statistically significant ( $P < 0.05$ , 0.01,

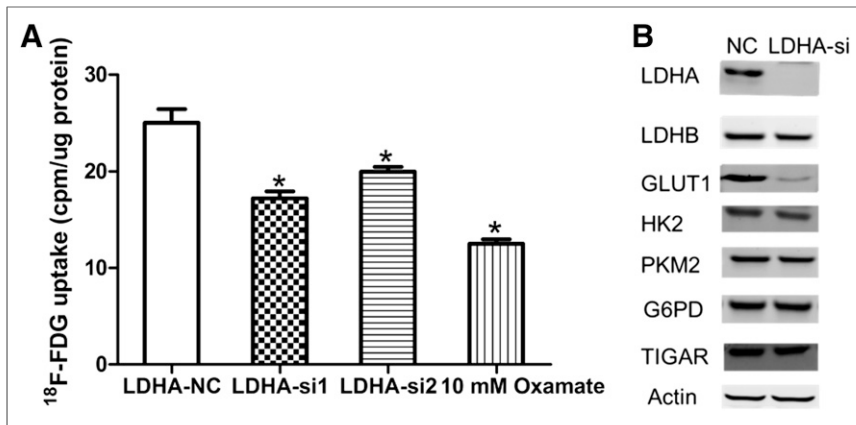


**FIGURE 3.** Influence of inhibition of LDHA on <sup>18</sup>F-FDG uptake, glycolytic enzymes, and glucose transporters in A549 cells. (A) Influence of LDHA siRNA or oxamate on <sup>18</sup>F-FDG uptake in A549 cells. A549 cells were transfected with control siRNA, LDHA siRNA, or oxamate. Two days later, A549 cells were incubated in DMEM with <sup>18</sup>F-FDG for 1 h, and uptake radioactivity was measured using well  $\gamma$  counter. (B) Influence of LDHA siRNA or oxamate on glycolytic enzymes and glucose transporters in A549 cells. All data represent mean  $\pm$  SEM of 3 independent experiments. NC = negative control. \* $P < 0.05$ .

and 0.001). All statistical analysis was performed using SPSS (version 13.0; SPSS Inc.).

## RESULTS

### Correlation Between $SUV_{max}$ and LDHA Expression

To investigate LDHA expression in patients with lung adenocarcinomas, we performed immunohistochemical staining on 51 lung adenocarcinoma cases. Table 1 shows the clinicopathologic characteristics and the correlations of LDHA expression to clinical factors. LDHA immunoreactivity was readily detected in the cytoplasm and occasionally in the nucleus (Fig. 1A). Patients were classified into 2 groups in terms of immunohistochemical staining for LDHA: patients with high LDHA expression (score 2 or 3,  $n = 26$ ) and patients with low LDHA expression (score 0 or 1,  $n = 25$ ). No significant differences between these 2 groups were found in terms of age, sex, N category, and M category. However, a significant difference in  $SUV_{max}$ , histologic type, T category, and primary tumor size was found between these 2 groups ( $P < 0.05$ ) (Table 1). Namely,  $SUV_{max}$  was significantly higher in primary tumors with high expression of LDHA than in primary tumors with low expression of LDHA ( $10.1 \pm 4.3$  and  $7.0 \pm 4.5$ , respectively;  $P = 0.018$ ). In Kaplan–Meier analysis, 5-y patient

survival was significantly lower in high-LDHA-expression than low-LDHA-expression tumors (Fig. 1B, 57.7% vs. 84.0%, log-rank  $P = 0.039$ ).

### Correlation Between <sup>18</sup>F-FDG Accumulation, LDHA Expression, GLUT1 Expression, and HK2 Expression

GLUT1 and HK2 expression were investigated by immunohistochemical analysis of the 51 primary tumors (Figs. 2A and 2B). Quantitatively, GLUT1 expression in primary tumors was positively correlated with  $SUV_{max}$  (Fig. 2C) whereas HK2 expression was not (Fig. 2D).  $SUV_{max}$  was significantly higher in tumors with high GLUT1 expression ( $n = 19$ ;  $11.3 \pm 4.6$ ) than tumors with low GLUT1 expression ( $n = 32$ ;  $6.9 \pm 3.8$ ;  $P < 0.01$ ). In addition, a significant correlation was confirmed between LDHA expression and GLUT1 expression ( $P = 0.005$ ) but not between

LDHA expression and HK2 expression ( $P = 0.65$ ; Supplemental Table 1 [supplemental materials are available at <http://jnm.snmjournals.org>]). These results can suggest that LDHA increases <sup>18</sup>F-FDG accumulation into non-small cell lung cancer, possibly by upregulation of GLUT1 expression but not HK2 expression.

### Effect of Knockdown of LDHA on Cellular <sup>18</sup>F-FDG Uptake

We performed <sup>18</sup>F-FDG uptake and lactate production assays to determine whether decreased LDHA had an effect on metabolic flux. <sup>18</sup>F-FDG uptake was significantly decreased after LDHA siRNA transfection in A549 cells (Fig. 3A). Oxamate, a specific LDH inhibitor, also decreased <sup>18</sup>F-FDG uptake in A549 cells. LDHA silencing and oxamate also decreased lactate production in A549 cells (Supplemental Fig. 1). In hypoxic conditions, the decrease in <sup>18</sup>F-FDG uptake was further enhanced in LDHA siRNA A549 cells (Supplemental Fig. 2). To further elucidate the mechanism of reduced glycolysis, we investigated whether LDHA knockdown affects the expression of other glycolytic enzymes such as LDHB (lactate dehydrogenase B), HK2, PKM2 (pyruvate kinase M2), TIGAR (Tp53-induced glycolysis and apoptosis regulator), G6PD (glucose-6-phosphate dehydrogenase), and glycolytic transporter GLUT1 (Fig. 3B). We found that there was a significant decrease in GLUT1 expression after LDHA knockdown in A549 cells.

### Effect of Downregulation of LDHA on Proliferation and Chemosensitivity In Vitro

We tested the effect of LDHA knockdown on the growth of A549 cells. It was found that LDHA knockdown and oxamate significantly inhibited ATP production and the proliferation of A549 cells (Figs. 4A and 4B;  $P < 0.001$ ). Because hypoxic regions in tumors must rely on glycolysis, we asked whether cells with knockdown of LDHA expression versus control cells would behave differently in hypoxic conditions.

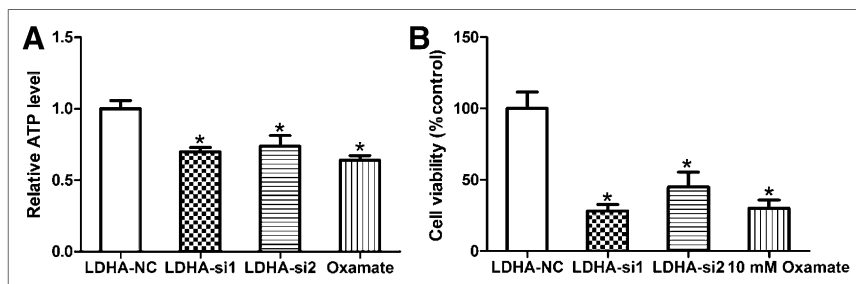


**FIGURE 4.** Influence of inhibition of LDHA on cellular ATP production and proliferation response in A549 cells. (A) Influence of LDHA siRNA or oxamate on cellular ATP production in A549 cells. (B) Influence of LDHA siRNA or oxamate on cellular proliferation in A549 cells. All data represent mean  $\pm$  SEM of 3 independent experiments. NC = negative control. \* $P < 0.05$ .

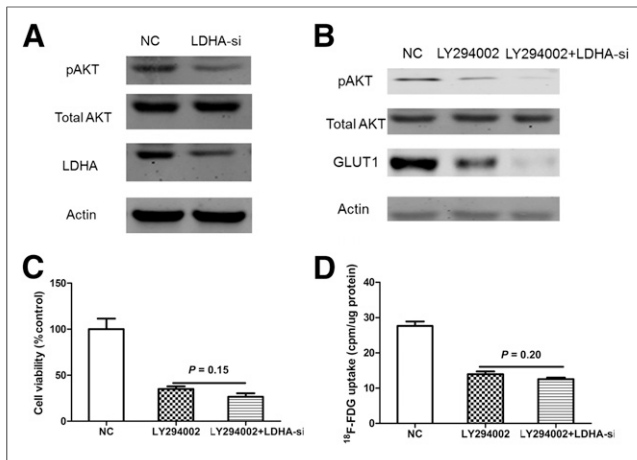


**FIGURE 5.** LDHA may increase  $^{18}\text{F}$ -FDG uptake via AKT-GLUT1 pathway in A549 cells. (A) Effects of LDHA knockdown on AKT phosphorylation. Activated form of AKT (pAKT) was significantly decreased after knockdown of LDHA. (B) Western blot analysis of pAKT and GLUT1 levels in LY294002-treated A549 cells transfected with LDHA-si1. (C) Influence of LDHA siRNA on cellular viability in LY294002-treated A549 cells. (D) Influence of LDHA siRNA on  $^{18}\text{F}$ -FDG uptake in LY294002-treated A549 cells. All data represent mean  $\pm$  SEM of 3 independent experiments. NC = negative control.

The decrease in ATP production and cell viability was further enhanced by 1% hypoxia (Supplemental Figs. 3A and 3B). When we treated the cell lines with the anticancer agent, we found that A549 cells were more sensitive to paclitaxel treatment in the LDHA knockdown (A549-siLDHA) cells than the scrambled control (LDHA-sc) cells, with an IC<sub>50</sub> of 12  $\mu\text{g}/\text{L}$  versus 8  $\mu\text{g}/\text{L}$ , respectively (Supplemental Fig. 4A). We used another commonly used clinical drug, cisplatin, and compared the cytotoxicity of A549-siLDHA and A549-sc cells with this drug. We obtained an IC<sub>50</sub> value of 3.5  $\mu\text{g}/\text{mL}$  for A549-sc cells versus 2  $\mu\text{g}/\text{mL}$  for A549-siLDHA cells (Supplemental Fig. 4B), also implying that LDHA knockdown increased drug sensitivity.

#### Molecular Mechanisms of Knockdown of LDHA Related to Cellular Inhibition and Reduced GLUT1

Because AKT is known to play an important role in cellular proliferation and activating the glucose transporter GLUT1 (25,26), we measured the expression of AKT after the cells were treated with LDHA siRNA transfection for 48 h. A549-siLDHA cells, compared with A549-sc cells, showed reduced expression of phosphorylated AKT (Fig. 5A).

We then applied the interruption approach to confirm whether pAKT is required for LDHA to modulate cellular proliferation and the expression of GLUT1. A549 cells were treated with LY294002 (AKT inhibitor), then transfection of LDHA-siRNA was performed using lipo2000 transfection reagent (Invitrogen). We found that treatment of LY294002 (10  $\mu\text{M}$ ) induced reduction of the pAKT level (Fig. 5B), cell viability (Fig. 5C), and  $^{18}\text{F}$ -FDG uptake (Fig. 5D), whereas knockdown of LDHA no longer distinctly affected these parameters. Together, the results from Figure 5 suggest that LDHA may modulate cellular proliferation,  $^{18}\text{F}$ -FDG uptake via the AKT-GLUT1 pathway.

#### DISCUSSION

$^{18}\text{F}$ -FDG PET/CT is a molecular imaging technique widely used for diagnosis, treatment response monitoring, surveillance, and

prognostication of a variety of cancers. However, the underlying mechanism for elevated  $^{18}\text{F}$ -FDG accumulation in malignant tumors is multifactorial and more complex than it may appear at first glance (15,27). This study shows that  $\text{SUV}_{\text{max}}$  is significantly higher in high-LDHA-expression tumors than low-LDHA-expression tumors, indicating that, in lung adenocarcinomas,  $^{18}\text{F}$ -FDG accumulation might reflect LDHA expression.

Studies have shown that  $^{18}\text{F}$ -FDG accumulation in human cancer cells depends mainly on glucose transporters (GLUTs) and hexokinases (15). The GLUT is the first rate-limiting step for glycolysis that transports  $^{18}\text{F}$ -FDG into the cell (28,29). Hexokinases bound to the outer membrane of mitochondria (30) and phosphorylated  $^{18}\text{F}$ -FDG to FDG-6-phosphate, which does not undergo further glycolytic pathways (15). The overexpression of GLUT1 is common in primary lung tumors and correlates with tumor differentiation grade, tumor stages, and prognosis (28). The overexpression of hexokinase has also been implicated in many cancers (31,32). Though the underlying reason for elevated  $^{18}\text{F}$ -FDG accumulation remains uncertain, some researchers have suggested that  $^{18}\text{F}$ -FDG accumulation depends especially on GLUT1 rather than glycolytic enzyme hexokinases in colorectal cancer (15,33). Consistent with these reports, our study demonstrated that GLUT1 expression was correlated with  $\text{SUV}_{\text{max}}$  whereas HK2 expression was not in lung adenocarcinomas.

It has been proposed that the increased acid production may be the underlying basis for promoting tumor survival and spread. The glycolytic enzyme LDHA, which converts pyruvate to lactate, ensures efficient glycolytic metabolism and plays an important role in the development, invasion, and metastasis of malignancies (20–22). Therefore, we evaluated whether LDHA knockdown or LDH inhibitor oxamate decreases  $^{18}\text{F}$ -FDG uptake and how it may affect cellular growth and proliferation. In this study, we confirmed that knockdown of LDHA significantly decreased  $^{18}\text{F}$ -FDG uptake. In in vitro assays, knockdown of LDHA led to a significant decrease in GLUT1 whereas other glycolytic enzymes were not changed remarkably. Thus, LDHA caused  $^{18}\text{F}$ -FDG accumulation possibly by upregulation of GLUT1 expression mainly but not HK2 expression. Consistent with in vitro study, our clinical study showed that LDHA expression correlated with expression of GLUT1 but not HK2. Primary tumors with high LDHA expression showed about a 1.44-fold increase in  $\text{SUV}_{\text{max}}$ , compared with those with low LDHA expression ( $P < 0.01$ ).

Many human malignant tumors have higher LDHA levels than normal tissues (19). There are several mechanisms of high LDHA expression in malignancies. In particular, LDHA could be regulated by c-Myc and hypoxia-inducible factor-1 at the transcriptional level (20,34). These transcription factors induce overexpression of LDHA, an increase in glucose consumption for conversion to lactate, cellular proliferation, and poor response to the anticancer treatment. In this study, LDHA inhibition led to decreased  $^{18}\text{F}$ -FDG uptake and inhibition of tumor growth both in vitro and in vivo. Knockdown of LDHA also caused a higher sensitivity to anticancer treatment than the scrambled control cells.

The mechanisms of carcinogenesis of LDHA have been extensively investigated. It has been known that LDHA plays an important role in glycolysis whereas inhibition of glycolysis causes a depletion of cellular ATP and leads to blockage of cell cycle progression and cell death (20–22). However, the molecular mechanism of the knockdown of LDHA that links cellular inhibition and reduced  $^{18}\text{F}$ -FDG uptake remains unclear. Oncogenic activation of AKT could promote tumor progression, increase glycolysis, and activate the glucose transporter GLUT1 (25,26). In this study, downregulation of the expression

of LDHA inhibited the activation of AKT (pAKT), thus leading to the inhibition of cellular growth and the reduction of GLUT1 expression and <sup>18</sup>F-FDG uptake (Supplemental Fig. 5).

## CONCLUSION

This study demonstrates that <sup>18</sup>F-FDG accumulation in primary lung adenocarcinomas is correlated with the expression of LDHA, and LDHA may modulate <sup>18</sup>F-FDG uptake through the LDHA–AKT–GLUT1 signaling. Moreover, glycolysis is closely associated with cellular proliferation and drug resistance in cancer cells, which is regulated by the expression of LDHA. The knockdown of LDHA inhibited cellular proliferation and increased drug sensitivity of cancer cells. These results indicate that <sup>18</sup>F-FDG PET/CT may predict LDHA expression levels and thus it can be used for noninvasive determination of therapeutic strategies using LDHA inhibitor in treating patients with lung adenocarcinomas.

## DISCLOSURE

The costs of publication of this article were defrayed in part by the payment of page charges. Therefore, and solely to indicate this fact, this article is hereby marked “advertisement” in accordance with 18 USC section 1734. Financial support was received from the National Natural Science Foundation of China (nos. 30830038, 30970842, 81071180, 81471685, 81471687, and 81471708), the Major State Basic Research Development Program of China (973 Program) (no. 2012CB932604), and the New Drug Discovery Project (no. 2012ZX09506-001-005). No other potential conflict of interest relevant to this article was reported.

## ACKNOWLEDGMENTS

We thank Dr. Yaer Hu of Shanghai Jiao Tong University School of Medicine for her assistance in isotopic tracing analysis. We thank Jun Zhao of Shanghai Huashan Hospital for his assistance in collection of clinical data and immunohistochemical analysis.

## REFERENCES

1. Tammemagi MC, Lam S. Screening for lung cancer using low dose computed tomography. *BMJ*. 2014;348:g2253.
2. Jemal A, Bray F, Center MM, et al. Global cancer statistics. *CA Cancer J Clin*. 2011;61:69–90.
3. Subramanian J, Govindan R. Lung cancer in never smokers: a review. *J Clin Oncol*. 2007;25:561–570.
4. Vansteenkiste J, De Ruysscher D, Eberhardt WE, et al. Early and locally advanced non-small-cell lung cancer (NSCLC): ESMO clinical practice guidelines for diagnosis, treatment and follow-up. *Ann Oncol*. 2013;24(suppl 6):vi89–vi98.
5. McElnay P, Lim E. Adjuvant or neoadjuvant chemotherapy for NSCLC. *J Thorac Dis*. 2014;6:S224–S227.
6. Kelsey CR, Light KL, Marks LB, et al. Patterns of failure after resection of non-small-cell lung cancer: implications for postoperative radiation therapy volumes. *Int J Radiat Oncol Biol Phys*. 2006;65:1097–1105.
7. Mountain CF. Revisions in the international system for staging lung cancer. *Chest*. 1997;111:1710–1717.
8. van Rens MT, de la Riviere AB, Elbers HR, et al. Prognostic assessment of 2,361 patients who underwent pulmonary resection for non-small cell lung cancer, stage I, II, and IIIA. *Chest*. 2000;117:374–379.

9. Watanabe Y. TNM classification for lung cancer. *Ann Thorac Cardiovasc Surg*. 2003;9:343–350.
10. Miller TR, Pinkus E, Dehdashti F, et al. Improved prognostic value of <sup>18</sup>F-FDG PET using a simple visual analysis of tumor characteristics in patients with cervical cancer. *J Nucl Med*. 2003;44:192–197.
11. Franzius C, Bielack S, Flege S, et al. Prognostic significance of <sup>18</sup>F-FDG and <sup>99m</sup>Tc-methylene diphosphonate uptake in primary osteosarcoma. *J Nucl Med*. 2002;43:1012–1017.
12. Siva S, Byrne K, Seel M, et al. <sup>18</sup>F-FDG PET provides high-impact and powerful prognostic stratification in the staging of Merkel cell carcinoma: a 15-year institutional experience. *J Nucl Med*. 2013;54:1223–1229.
13. Pieterman RM, van Putten JW, Meuzelaar JJ, et al. Preoperative staging of non-small-cell lung cancer with positron-emission tomography. *N Engl J Med*. 2000;343:254–261.
14. Antoniou AJ, Marcus C, Tahari AK, et al. Follow-up or surveillance <sup>18</sup>F-FDG PET/CT and survival outcome in lung cancer patients. *J Nucl Med*. 2014;55:1062–1068.
15. Jadvar H, Alavi A, Gambhir SS. <sup>18</sup>F-FDG uptake in lung, breast, and colon cancers: molecular biology correlates and disease characterization. *J Nucl Med*. 2009;50:1820–1827.
16. Higashi T, Saga T, Nakamoto Y, et al. Relationship between retention index in dual-phase <sup>18</sup>F-FDG PET, and hexokinase-II and glucose transporter-1 expression in pancreatic cancer. *J Nucl Med*. 2002;43:173–180.
17. Warburg O. On the origin of cancer cells. *Science*. 1956;123:309–314.
18. Gatenby RA, Gillies RJ. Why do cancers have high aerobic glycolysis? *Nat Rev Cancer*. 2004;4:891–899.
19. Miao P, Sheng S, Sun X, et al. Lactate dehydrogenase A in cancer: a promising target for diagnosis and therapy. *IUBMB Life*. 2013;65:904–910.
20. Fantin VR, St-Pierre J, Leder P. Attenuation of LDH-A expression uncovers a link between glycolysis, mitochondrial physiology, and tumor maintenance. *Cancer Cell*. 2006;9:425–434.
21. Sheng SL, Liu JJ, Dai YH, et al. Knockdown of lactate dehydrogenase A suppresses tumor growth and metastasis of human hepatocellular carcinoma. *FEBS J*. 2012;279:3898–3910.
22. Le A, Cooper CR, Gouw AM, et al. Inhibition of lactate dehydrogenase A induces oxidative stress and inhibits tumor progression. *Proc Natl Acad Sci USA*. 2010;107:2037–2042.
23. Yu Z, Ge Y, Xie L, et al. Using a yeast two-hybrid system to identify FTCD as a new regulator for HIF-1α in HepG2 cells. *Cell Signal*. 2014;26:1560–1566.
24. Yang W, Zheng Y, Xia Y, et al. ERK1/2-dependent phosphorylation and nuclear translocation of PKM2 promotes the Warburg effect. *Nat Cell Biol*. 2012;14:1295–1304.
25. Robey RB, Hay N. Is Akt the “Warburg kinase”? Akt-energy metabolism interactions and oncogenesis. *Semin Cancer Biol*. 2009;19:25–31.
26. Chan CH, Li CF, Yang WL, et al. The Skp2-SCF E3 ligase regulates Akt ubiquitination, glycolysis, hereceptin sensitivity, and tumorigenesis. *Cell*. 2012;149:1098–1111.
27. Miles KA, Williams RE. Warburg revisited: imaging tumour blood flow and metabolism. *Cancer Imaging*. 2008;8:81–86.
28. Medina RA, Owen GI. Glucose transporters: expression, regulation and cancer. *Biol Res*. 2002;35:9–26.
29. Macheda ML, Rogers S, Best JD. Molecular and cellular regulation of glucose transporter (GLUT) proteins in cancer. *J Cell Physiol*. 2005;202:654–662.
30. Gottlob K, Majewski N, Kennedy S, et al. Inhibition of early apoptotic events by Akt/PKB is dependent on the first committed step of glycolysis and mitochondrial hexokinase. *Genes Dev*. 2001;15:1406–1418.
31. Wolf A, Agnihotri S, Micallef J, et al. Hexokinase 2 is a key mediator of aerobic glycolysis and promotes tumor growth in human glioblastoma multiforme. *J Exp Med*. 2011;208:313–326.
32. Palmieri D, Fitzgerald D, Shreeve SM, et al. Analyses of resected human brain metastases of breast cancer reveal the association between up-regulation of hexokinase 2 and poor prognosis. *Mol Cancer Res*. 2009;7:1438–1445.
33. Kawada K, Nakamoto Y, Kawada M, et al. Relationship between <sup>18</sup>F-fluorodeoxyglucose accumulation and KRAS/BRAF mutations in colorectal cancer. *Clin Cancer Res*. 2012;18:1696–1703.
34. Shim H, Dolde C, Lewis BC, et al. c-Myc transactivation of LDH-A: implications for tumor metabolism and growth. *Proc Natl Acad Sci USA*. 1997;94:6658–6663.